Scripta Materialia 149 (2018) 40–43

Contents lists available at ScienceDirect

Scripta Materialia

journal homepage: www.elsevier.com/locate/scriptamat

Regular article

Direct *in situ* observation of toughening mechanisms in nanocomposites of silicon nitride and reduced graphene-oxide

Cristina Ramírez [a], Qizhong Wang [a], Manuel Belmonte [b], Pilar Miranzo [b], M. Isabel Osendi [b], Brian W. Sheldon [a], Nitin P. Padture [a,*]

[a] School of Engineering, Brown University, Providence, RI 02912, USA
[b] Institute of Ceramics and Glass (ICV), CSIC, 28049 Madrid, Spain

ARTICLE INFO

Article history:
Received 22 October 2017
Received in revised form 2 February 2018
Accepted 2 February 2018
Available online xxxx

Keywords:
Silicon nitride
Graphene
Graphene oxide
Ceramic
Nanocomposite
Toughening

ABSTRACT

In situ observations are performed, for the first time, of stable crack propagation in nanocomposites of silicon nitride (Si_3N_4) and reduced graphene-oxide (rGO) inside a scanning-electron microscope. Two different specimen geometries (wedge-splitting and double-cantilever beam) are used to observe crack interactions with rGO stacks in two different orientations (cross-section and in-plane). These observations provide new insights into the unique, effective pull-out of crack-bridging rGO stacks, which appears to be responsible for the extraordinary toughness in the Si_3N_4/rGO nanocomposites. These insights could be used to design and create future ceramic/rGO nanocomposites with superior mechanical properties.

There has been great interest in using carbon nanostructures, especially one-dimensional (1-D) carbon nanotubes (CNTs), to toughen brittle ceramics (see recent reviews [1,2]). This is because CNTs have a set of exceptional structural features and properties that are not found in conventional ceramic reinforcements such as platelets, whiskers, or fibers. Accordingly, the toughening mechanisms in ceramic/CNTs nanocomposites are also unique [3,4]. With the advent of 2-D graphene and its derivatives, which also have a set of unprecedented structural features and properties, it is a natural progression to use them as reinforcements in ceramic nanocomposites. (The term 'graphene' refers to flexible few-layer graphene stacks, in addition to single-sheet graphene, but not stiff graphite 'platelets.') We argue that the 2-D nature of both the graphene reinforcements, and the crack that these reinforcements are expected to bridge, is likely to make graphene a more effective reinforcement compared to the 1-D CNTs. Early reports showed significant toughening in alumina (Al_2O_3) [5] and silicon nitride (Si_3N_4) [6] ceramics with the introduction of graphene reinforcements in the form of reduced graphene oxide (rGO) stacks. Since then, there have been numerous reports showing toughening in a wide variety of ceramic/graphene nanocomposites [7,8]. There is, however, large variation in toughness gains, which can be attributed to large variation in the processing and the microstructures. Generally, rGO stacks are found to be more effective because of the better dispersion of hydrophilic GO containing surface functional groups (O^-, OH^-, $COOH^-$) in the initial GO/ceramic powder mixture, as opposed to non-functionalized hydrophobic graphene [9]. While GO typically has inferior mechanical properties such as elastic modulus and strength, graphene-like behavior can be recovered by reducing the GO (rGO) during heat-treatments as part of the composite densification processes such as spark-plasma sintering (SPS) [10]. Furthermore, the functional groups on the starting GO surfaces can promote better interfacial adhesion between the outer layers of the rGO stacks and the ceramic surfaces [11].

While most of the relevant studies report toughness values, measured using either bend or indentation tests, some also provide micrographs of static cracks that show bridging by rGO stacks in the wake of the crack tip and/or on fracture surfaces [6–8,12]. Toughening mechanisms are then speculatively proposed based on those observations. In this context, it is well established that *in situ* observations of crack propagation provides significantly deeper insight into the toughening mechanisms in other materials [4,13,14]. To that end, direct *in situ* investigation of crack propagation in fully-dense SPSed Si_3N_4/rGO nanocomposites were performed for the first time, to provide new insights into the unique toughening mechanisms that operate in these types of materials. Note that Si_3N_4 is perhaps one of the most widely studied ceramic matrix in the context of incorporating graphene fillers because of the high toughness levels achieved in the resulting nanocomposites [8,17]. Two different specimen geometries (Fig. 1A and B) are used to enable stable crack growth during loading in a micro-test device, inside of a scanning electron microscope (SEM): (i) wedge-splitting [15], and

* Corresponding author.
E-mail address: nitin_padture@brown.edu (N.P. Padture).

https://doi.org/10.1016/j.scriptamat.2018.02.004
1359-6462/

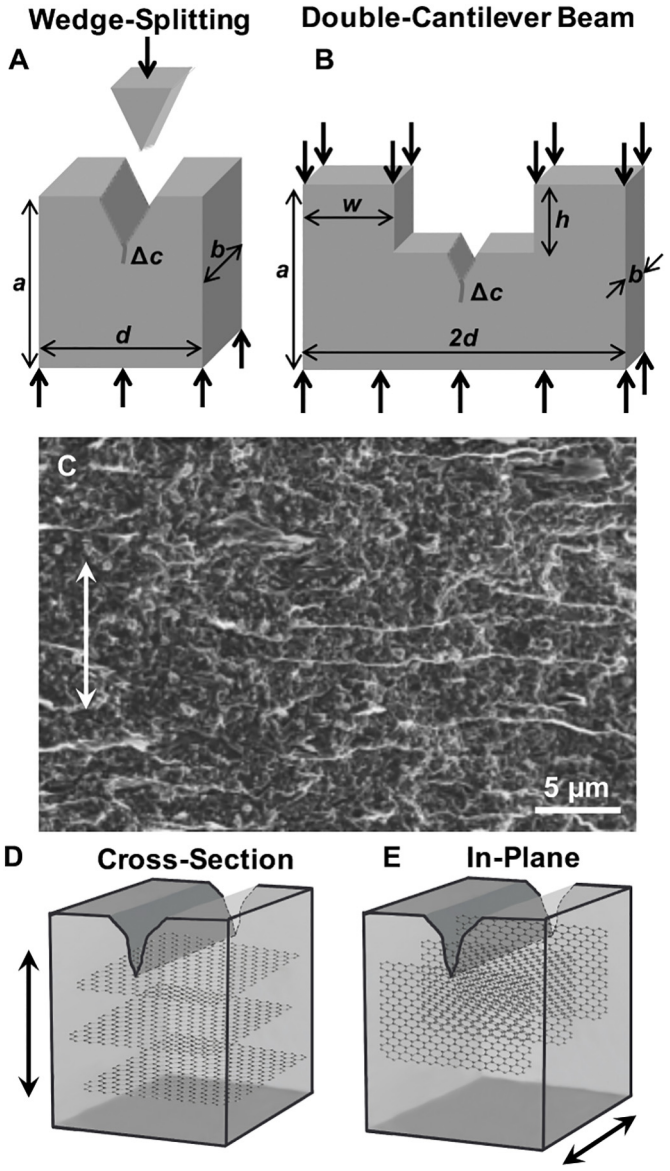

Fig. 1. *In situ* test specimen geometries used to obtain stable crack propagation inside the SEM: (A) wedge-splitting ($a = 10$ mm, $b = 3$ mm, $d = 5$ mm) and (B) DCB in compression ($a = 4.8$ mm for in-plane, 3 mm for cross-section, $b = 1$ mm, $d = 1.9$ mm, $h = 0.6$ mm, $w = 1.2$ mm). (C) SEM micrograph of fracture surface of Si_3N_4/rGO nanocomposite (arrow indicates SPS pressing direction). Schematic depiction of the rGO-stacks orientation with respect to the main crack (arrows indicate SPS pressing direction): (D) cross-section and (E) in-plane.

(ii) double-cantilever beam (DCB) in compression [16]. The SPSed nanocomposite pellets are unintentionally orthotropic, where most of the rGO stacks naturally align in planes perpendicular to the SPS pressure axis. Fig. 1C is a cross-sectional SEM micrograph of Si_3N_4/rGO nanocomposite showing this alignment of rGO stacks. This presents a unique opportunity to study crack propagation in two different orientations: 'cross-section' (Fig. 1D) and 'in-plane' (Fig. 1E), where the rGO stacks are 'normal' and 'edge-on', respectively, with respect to the planar crack front.

Fully-dense SPSed Si_3N_4/rGO nanocomposite pellets (3 mm thickness, 20 mm diameter) from a previous study [17] are used here. They contain 4.3 vol% rGO (Fig. 1C), with an impressive toughness of ~10 MPa·$m^{0.5}$ in the 'cross-section' orientation, as measured using the reliable surface-crack in flexure (SCF) toughness test [18]. This represents over two-fold increase in the toughness compared to monolithic Si_3N_4 ceramic (~4.5 MPa·$m^{0.5}$) without the rGO. (See Refs. [10,17] for details regarding processing, microstructures, and mechanical properties.) Both types of specimens were cut from the same pellets in the two orientations using a low-speed diamond saw, followed by surface-polishing. A piezo-driven micro-test device (MT10141, Deben, Woolpit, UK) with specially fabricated fixtures, equipped with a load cell (2 kN capacity), was used to load the test specimens in compression (Fig. 1A and B) [4]. In both types of specimens, sharp 'V' notches were cut using a razorblade with a 1-μm diamond suspension. Compression was applied to propagate a sharp, stable crack (Δc) at the root of the 'V' notch. The load was then increased and held, allowing us to photograph the crack using secondary-electron imaging in the SEM. This process was repeated at successively higher applied loads. There are pros and cons to the two specimen geometries. While the crack growth is more stable in the DCB geometry, it requires much larger loads (~2 kN), limiting the dimensions of DCB specimens. As mentioned earlier, the specimens are oriented in two different ways. Both specimen geometries (wedge-splitting and DCB) are used in the in-plane orientation (Fig. 1E), but only wedge-splitting specimen geometry is used for cross-section orientation (Fig. 1D) due to the limitation on the thickness (3 mm) of the available pellets.

Fig. 2A–D are a sequence of SEM micrographs taken from a fixed location at different loads as the main crack tip propagates (downward) using the DCB geometry (Fig. 1B) in the cross-section orientation (see Fig. 1D; horizontal rGO stacks are perpendicular to the plane of the image). In Fig. 2A it can be seen that thinner rGO-stack bridges (upper) have already pulled-out and fractured. The thicker rGO-stack bridge is still intact (lower). With increasing horizontal crack-wall separation (downward main-crack propagation), the rGO stack appears to stretch thin and split along the weak rGO layers, resulting in sliding between the layers (Fig. 2B and C). The rGO stack thins further, bends, and eventually fractures (Fig. 2D). (Note that there is always some vertical displacement of the crack walls during crack propagation, resulting in the rGO bending.) However, in all of the SEM images (Fig. 2A–D), there is no relative motion between the Si_3N_4 matrix and the embedded rGO stack within the composite on either side of the crack. Instead, the rGO stack appears to be anchored strongly within the Si_3N_4 matrix. This implies the absence of classical pull-out mechanism observed in toughened ceramics, where the bridging reinforcement (*e.g.* platelet, whisker, fiber) slides out frictionally, leaving behind an empty socket [13]. This type of non-classical pull-out behavior is found to be pervasive in the Si_3N_4/rGO nanocomposite in the cross-section orientation. Another example of a sequence of *in situ* SEM micrographs in cross-section orientation (wedge-splitting geometry) is presented as a movie in Supplementary Information (SI) showing very similar behavior. Thus, these results show that the unique 2-D layered structure of the rGO stacks results in pull-out *via* a fundamentally different mechanism.

Now consider the in-plane orientation (see Fig. 1E), where rGO stacks are in the plane of the image. Figs. 2E–H show a sequence of SEM micrographs taken from a fixed location as the crack walls separate using the wedge-splitting geometry. The main crack tip (front) intersects the large rGO stack edge-on when it first encounters it in this orientation. Here, it appears that the rGO stack is tough enough to resist fracture as the crack walls separate and the main crack tip propagates downward through the matrix. The stretching and narrowing of the rGO-stack width is dramatic going from Fig. 2E to G, which confirms that the rGO stack is anchored strongly within the Si_3N_4 matrix. As the cracks walls separate, the rGO stack narrows further and eventually fractures, most likely from an edge flaw (arrow). Here also, the rGO stack does not appear to pull-out *via* the classical mechanism. (See SI for a video of this sequence of SEM micrographs.) Another sequence of *in situ* SEM micrographs is shown in Fig. S1A–D (in-plane orientation, wedge-splitting geometry) in SI. Once again, stretching of a well-anchored rGO stack and its eventual fracture is observed.

In contrast, smaller rGO stacks appear to pull-out in a more classical manner, as seen in Fig. 2I–K (in-plane orientation, DCB geometry). The rGO stack does not appear to stretch with increasing crack-wall

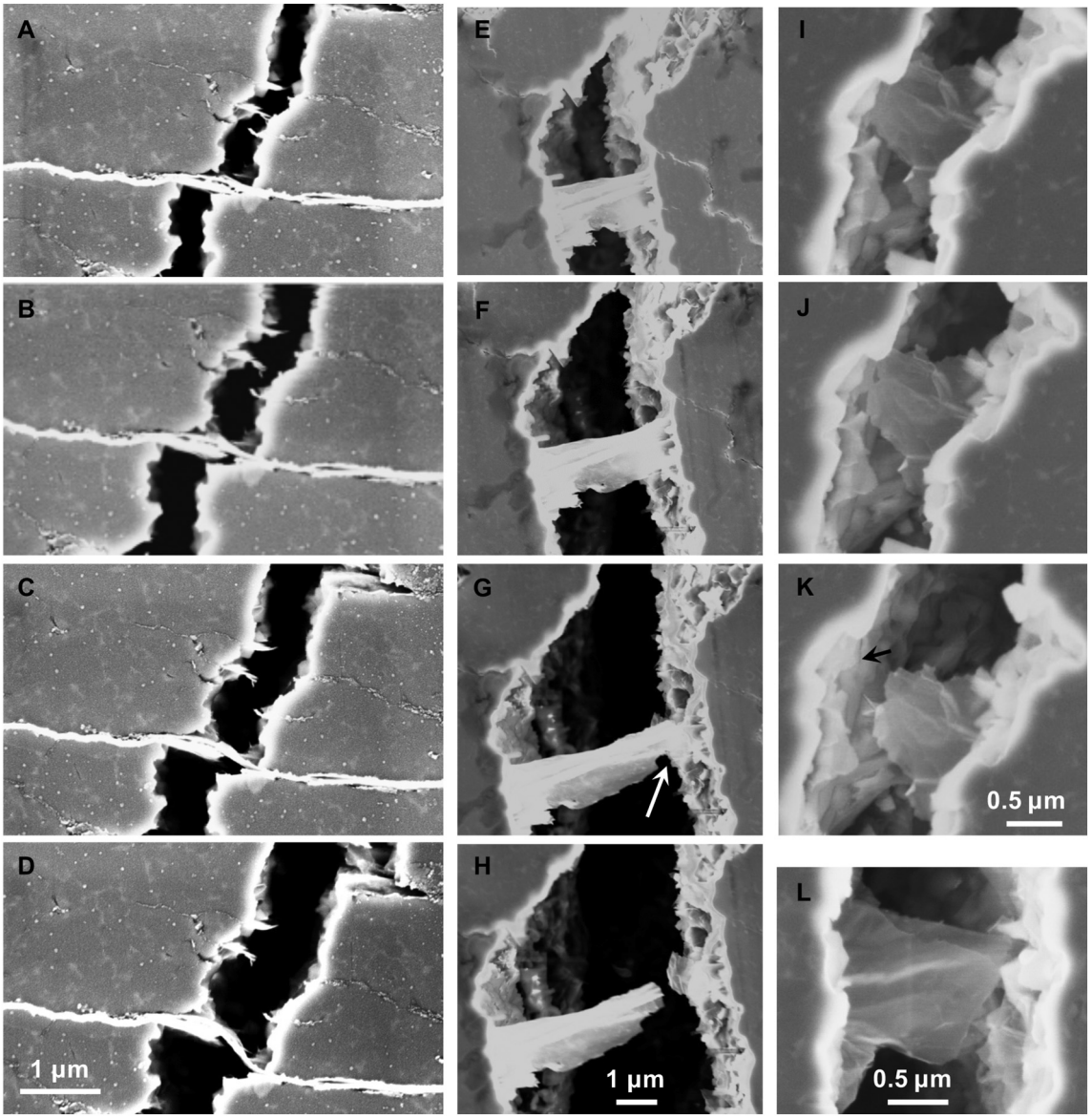

Fig. 2. Sequences of *in situ* SEM micrographs of fixed regions in the Si_3N_4/rGO nanocomposite as the crack walls separate (main crack-tip propagation downwards): (A–D) large rGO stack in cross-section orientation (DCB geometry), (E–H) large rGO stack in in-plane orientation (wedge-splitting geometry), and (I–K) small rGO stack in in-plane orientation (DCB geometry). (L) SEM micrograph of a pulled-out small rGO stack at the end of yet another *in situ* test (in-plane orientation, DCB geometry).

separation, and the empty socket left by the rGO-stack pullout is visible on the left in Fig. 2K (arrow). Fig. 2L is another example of a classically pulled-out smaller rGO stack from the socket (right) at the end of an *in situ* test (in-plane orientation, DCB specimen geometry).

It is clear that the larger rGO-stack crack-bridges are anchored strongly within the nanocomposite. The smaller rGO stacks pull-out classically, but their outer layers could still be bonded to the Si_3N_4 matrix inside the sockets. There is no evidence of the matrix material on the surfaces of pulled-out rGO stacks, small or large, which supports this hypothesis. (Note that the anisotropic thermal-expansion and elastic properties of the rGO stack within these nanocomposites are not known, and, therefore, the clamping residual stresses cannot be calculated reliably.) In addition to the strong chemical bonding, the larger rGO stacks are corrugated, and their aspect ratio (50 to 100) is also high (see Fig. 1C). This appears to be important for the anchoring of the rGO stacks within the Si_3N_4 matrix, in addition to the possible strong chemical bonding. Furthermore, unlike conventional brittle-ceramic reinforcements (platelets, whiskers, fibers), rGO stacks are highly flexible in bending and relatively 'ductile.' This assures that the larger rGO stacks do not fracture within the nanocomposite matrix prematurely, precluding classical pullout. Thus, the unique combination of features of the larger rGO stacks (surface corrugation, strong bonding to the matrix, flexibility, 'ductility') is responsible for the excceptional and effective crack-bridging behavior of these reinforcements in Si_3N_4/rGO nanocomposites [19].

Fig. 3 summarizes schematically the contrast between crack-wake bridging toughening of ceramics by conventional ceramic platelets and 2-D rGO stacks. Based on these new insights, the following design guidelines can be proposed for further improvements in the toughness of ceramic/rGO nanocomposites. First, adhesion between rGO-stack outer layers and the ceramic could be further improved through interfacial engineering. Second, residual stresses could be tailored to clamp the rGO-stacks. However, this will require detailed knowledge of the relations between the relevant properties (anisotropic thermal-expansion and elastic properties) of the rGO stacks and their structure. Finally, the rGO stacks could be made stronger with fewer defects, through better-controlled GO reduction protocols or other methods of dispersing high-quality graphene stacks in the nanocomposites.

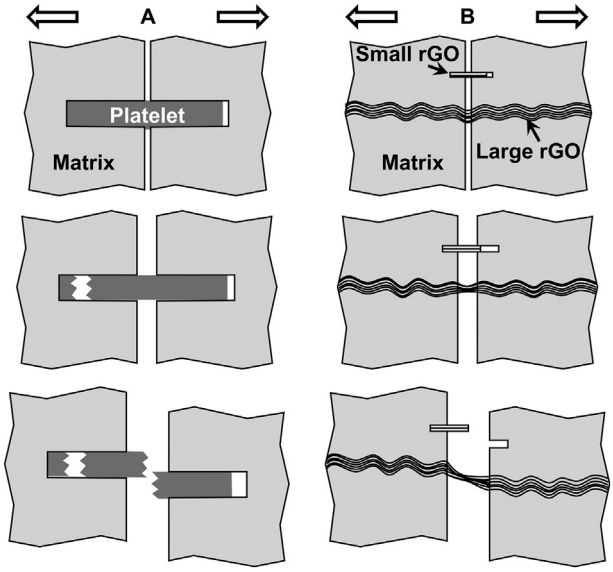

Fig. 3. Schematic illustration highlighting the contrast between crack-wake bridging toughening of ceramics by: (A) conventional brittle-ceramic platelet reinforcement and (B) small and large 2-D rGO stacks. Cross-section orientation. Crack walls separate horizontally (top to bottom), with some vertical displacement, as the main crack propagates downwards.

In summary, we have observed, *in situ* in the SEM, the propagation of stable cracks and their interaction with the rGO-stack reinforcements in orthotropic Si_3N_4/rGO nanocomposites in the in-plane and the cross-sectional orientations. It is found that smaller crack-bridging rGO stacks pull-out according to the classical mechanism seen in conventional platelet-reinforced composites. In contrast, larger rGO stacks, with their strong bonding to the matrix, corrugated nature, and very high aspect ratios, are anchored firmly within the Si_3N_4 matrix. This, combined with the flexible and 'ductile' nature of the larger rGO stacks, is responsible for the highly effective crack-wake bridging and the attendant extraordinary toughness in these Si_3N_4/rGO nanocomposites. These insights could be used to design and create future ceramic/rGO nanocomposites with even higher toughness.

Supplementary data to this article can be found online at https://doi.org/10.1016/j.scriptamat.2018.02.004.

Acknowledgements

We thank Ms. Y. Liu for her experimental assistance. Primary financial support for this research was provided by the U.S. Department of Energy, Office of Basic Energy Sciences, under Contracts DE-FG02-10ER46771 and DE-SC0018113. Q.W. and N.P.P. also acknowledge the generous gift from the II-VI Foundation. M.B., P.M., and M.I.O. acknowledge the financial support through the project MAT2015-67437-R (MINECO/FEDER, UE).

References

[1] E. Zapata-Solvas, D. Gómez-García, A. Domínguez-Rodríguez, J. Eur. Ceram. Soc. 32 (2012) 3001.
[2] A. Azarniya, S. Sovizi, A. Azarniya, M.R.R.T. Boyuk, T. Varol, P. Nithyadharseni, H.R.M. Hosseini, S. Ramakrishna, M.V. Reddy, Nano 9 (2017), 12779.
[3] N.P. Padture, Adv. Mater. 21 (2009) 1767.
[4] Y. Liu, C. Ramírez, L. Zhang, W. Wu, N.P. Padture, Acta Mater. 127 (2017) 203.
[5] K. Wang, Y. Wang, Z. Fan, J. Yan, T. Wei, Mater. Res. Bull. 46 (2011) 315.
[6] L.S. Walker, V.R. Marotto, M.A. Rafiee, N. Koratkar, E. Corral, ACS Nano 5 (2011) 3182.
[7] K. Markandan, J.K. Chin, M.T.T. Tan, J. Mater. Res. 32 (2017) 84.
[8] P. Miranzo, M. Belmonte, M.I. Osendi, J. Eur. Ceram. Soc. 37 (2017) 3649.
[9] S. Park, R.S. Ruoff, Nat. Nanotechnol. 4 (2009) 217.
[10] C. Ramírez, S.M. Vega-Diaz, A. Morelos-Gómez, F. Figueiredo, M. Terrones, M.I. Osendi, M. Belmonte, P. Miranzo, Carbon 57 (2013) 425.
[11] J. Wozniak, A. Jastrzebska, T. Cygan, A. Olszyna, J. Eur. Ceram. Soc. 37 (2017) 1587.
[12] R. Sedlák, A. Kovalcíková, E. Múdra, P. Rutkowski, A. Dubiel, V. Girman, R. Bystricky, J. Dusza, J. Eur. Ceram. Soc. 37 (2017) 3773.
[13] J. Rödel, E.R. Fuller Jr, B.R. Lawn, J. Am. Ceram. Soc. 74 (1991) 3154.
[14] A. Nieto, B. Boesl, A. Agarwal, Carbon 85 (2015) 299.
[15] H. Harmouth, Theor. Appl. Fract. Mech. 23 (1995) 103.
[16] L. Liu, Y. Wang, X. Li, L. Xu, X. Cao, Y. Wang, Z. Wang, C. Meng, W. Zhu, X. Ouyang, J. Am. Ceram. Soc. 99 (2016) 257.
[17] C. Ramírez, P. Miranzo, M. Belmonte, M.I. Osendi, P. Poza, S.M. Vega-Diaz, M. Terrones, J. Eur. Ceram. Soc. 34 (2014) 161.
[18] ASTM, C1421-01b. Annual Book of ASTM Standards, ASTM International, West Conshohocken, PA, 2007.
[19] C. Ramírez, M.I. Osendi, Ceram. Intl. 40 (2014) 11187.